Atomic and electronic structure of $Pd_{40}Ni_{40}P_{20}$ bulk metallic glass from *ab initio* simulations

Vijay Kumar,[1,*] T. Fujita,[2] K. Konno,[3] M. Matsuura,[4] M. W. Chen,[2] A. Inoue,[2] and Y. Kawazoe[4]

[1]*Dr. Vijay Kumar Foundation, 1969 Sector 4, Gurgaon 122001, Haryana, India*

[2]*WPI Advanced Institute for Materials Research, Tohoku University, 2-1-1 Katahira, Aoba-ku, Sendai 980-8577, Japan*

[3]*Miyagi National College of Technology, Natori 981-1239, Japan*

[4]*Institute for Materials Research, Tohoku University, 2-1-1 Katahira, Aoba-ku, Sendai 980-8577, Japan*

(Received 20 June 2011; revised manuscript received 7 August 2011; published 14 October 2011)

The atomic structure of $Pd_{40}Ni_{40}P_{20}$ bulk metallic glass has been simulated using an *ab initio* molecular dynamics method with projector-augmented wave pseudopotentials for electron-ion interaction and generalized gradient approximation for exchange-correlation energy. The calculated extended x-ray absorption fine structure (EXAFS) spectra of Pd-K and Ni-K edges, the mass density, and the electronic structure agree remarkably well with the available experimental data and the EXAFS spectra measured at the SPring-8 synchrotron radiation facility. Our results show that the atomic structure can be described in terms of P-centered polyhedra. There are no two P atoms that are nearest neighbors at this composition, and this could be a reason for the observed optimal P concentration of about 20 at.%. The neighboring polyhedra share metal (M) atoms and form a polar covalently bonded random network of P-M-P favoring certain angles. The remaining M atoms act as metallic glue with a tendency of nanoscale clustering of Pd-Pd and Ni-Ni atoms.

DOI: 10.1103/PhysRevB.84.134204 PACS number(s): 71.23.Cq, 71.15.Pd, 61.05.cj, 81.05.Kf

I. INTRODUCTION

A remarkable feat was achieved nearly two decades ago[1] when metallic glasses were developed in bulk form by low critical cooling rates ranging between 1 and 100 K/s. The first bulk metallic glass (BMG) was obtained[2] in the $Pd_{40}Ni_{40}P_{20}$ system with ingots of about 5 mm diameter. Since then, rapid experimental progress has shown[3] the existence of BMG phases in a large number of alloys with samples of up to about 10 cm diameter, in some cases, and also using slow cooling of even less than 1 K/s, similar to crystalline materials. This new macroscopic phase of matter has attractive properties for applications. It is harder than steel and has resistance to wear and corrosion. It has increased plasticity, though it is tougher than ceramics. However, its characterization is challenging since the most basic knowledge, namely, the atomic structure that determines most of the properties of materials, remains an open problem because of the inherent lack of periodicity, unlike in crystalline materials, for which atomic structure can be obtained in great detail even in the most complex cases. Here, we report[4] the results of *ab initio* simulations on Pd-Ni-P BMG, which has served well as a reference BMG for further developments. The calculated atomic structure and the electronic properties agree very well with the known experimental data, as well as our extended x-ray absorption fine structure (EXAFS) measurements.

Earlier attempts to understand the excellent glass-forming ability[5] of the $Pd_{40}Ni_{40}P_{20}$ ternary system include photoemission experiments,[6] which show significantly lower density of states (DOS) at the Fermi energy, E_F, compared with bulk Ni or bulk Pd. Nagel and Tauc[7] have suggested low DOS at the E_F to be a criterion for metallic glass formation. Measurements of the radial distribution function[8] have shown short- and medium-range orders in BMGs. Glassy materials have long been considered to have short-range order like in crystalline counterparts, and, in many cases, there have been indications of the existence of medium-range order. To understand their atomic structure, cluster models have been developed over a long period of time.[9] In recent years, the BMG phase has also been considered as an ensemble of atomic clusters.[10] However, such models need to be firmly established, such as for Zr-based alloys,[11,12] considering different BMGs and using *ab initio* calculations that have predictive capability and are feasible without any assumption of the existence of clusters or short-range order.

The paper is organized as follows. In Sec. II, we present the details of EXAFS measurements and the method of calculations, as well as the simulations. In Sec. III, we present our results, while in Sec. IV, we give a summary of our work.

II. EXPERIMENTAL AND CALCULATIONAL METHODS

We studied the atomic structure of $Pd_{40}Ni_{40}P_{20}$ BMG by EXAFS spectroscopy at the beam line BL01B1 of the SPring-8 synchrotron radiation facility in Japan. EXAFS spectra of Pd-K and Ni-K edges were measured in a transmission mode at a temperature of 20 $\pm$ 0.1 K. The thicknesses of the samples were optimized to obtain suitable absorption jumps at each K-absorption edge. The experimental EXAFS signals were extracted by a standard data-reduction procedure using the UWXAFS program.[13] Further, the $Pd_{40}Ni_{40}P_{20}$ BMG was simulated using an *ab initio* molecular dynamics method[14] in a microcanonical (NVE) ensemble with projector-augmented wave (PAW) pseudopotentials for electron-ion interactions[15] and a plane-wave basis set. Generalized gradient approximation[16] was used for the exchange-correlation energy. The simulation sample is represented by 250 atoms in a simple cubic cell with periodic boundary conditions. For such large unit cells, only the gamma point is used to perform Brillouin zone integrations. Four samples of BMG were simulated by taking different initial atomic configurations that were obtained by random distribution of 100 Pd, 100 Ni, and 50 P atoms in the unit cell and by giving different heat treatments. In each case, after the electronic wave functions were converged for the initial atomic configuration, the system was heated to the desired temperature and then cooled "slowly" in steps of

200 K. The total simulation time for each sample is in the range of 50–60 ps. In the following, we briefly give the history of different simulation samples.

A. Sample 1

The system was heated to 2000 K and then cooled until the temperature reached 300 K. Subsequently, the atomic structure was optimized to the nearest minimum by allowing relaxation of ionic positions as well as the size and shape of the unit cell. The resulting radial distribution function $g(r)$ at 0 K as well as the averaged $g(r)$ at 300 K showed a sharp peak at around 2.2 Å. Further reheating to 800 K and cooling did not change the $g(r)$ much.

B. Sample 2

The system was heated to 2400 K and cooled to 300 K, as above. Subsequently, the atomic structure was optimized by performing ionic as well as cell relaxations. This run led to the lowering of the energy and a decrease in the sharp peak in $g(r)$ at around 2.2 Å.

C. Samples 3 and 4

In two other independent runs, the system was heated at 3000 K and then cooled up to 300 K. One run was done starting from an initial random configuration (sample 3), and in another run (sample 4), the configuration obtained at 800 K for sample 2 was taken as the initial configuration. Similar to samples 1 and 2, the final structure was obtained by fully relaxing the atomic positions, cell shape, and volume. In both cases, the energy of the fully optimized sample was lower as compared to the other runs. However, sample 3 had the lowest energy. In the following, we present results derived from this sample.

III. RESULTS

A. Atomic structure

In Fig. 1(a), we show the optimized atomic structure obtained at zero temperature. It has the least volume, and its energy is lower by about 4 eV as compared to sample 1. Therefore, initial heating at higher temperature leads to a better mixing of atoms. The faster diffusion at the higher temperature of 3000 K, as well as longer simulation time, allowed the system to visit configurations that turned out to be lower in energy. The calculated density is 9.2 g/cm^3, and it compares very well with the experimental value[17] of 9.4 g/cm^3. Also, the averaged $g(r)$ at 300 K (Fig. 1) agrees well with the available experimental data[7] at room temperature. The optimized cell dimensions of a slightly deformed cubic cell are about 15 Å each, and we can expect $g(r)$ to be well represented up to a distance of about 6 Å, beyond which the periodic boundary conditions may affect its behavior. The EXAFS spectra of the simulated BMG were calculated using an *ab initio* code[18] implanted in FEFF8, and the results agree very well with our experimental data, as shown in Fig. 2. The cohesive energy of $Pd_{40}Ni_{40}P_{20}$ BMG from the atomic constituents is calculated to be 4.47 eV/atom. This is higher

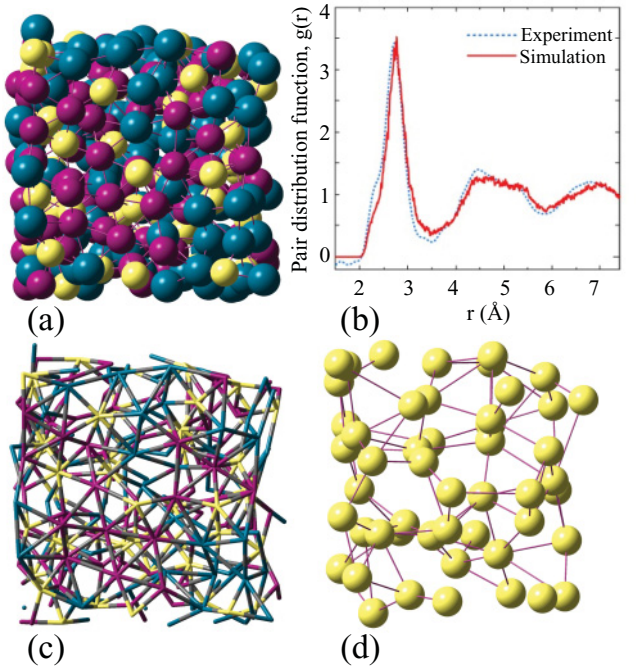

FIG. 1. (Color online) (a) Simulated atomic structure of $Pd_{40}Ni_{40}P_{20}$ BMG. Dark-blue (dark gray in print), violet (black in print), and yellow (light gray in print) balls represent Pd, Ni, and P atoms, respectively. (b) Comparison of the calculated averaged pair distribution function at 300 K with the experimental results at room temperature taken from Ref. 8. (c) A frame of the atomic structure showing P-Ni and P-Pd connections that are dominant. No two P atoms are nearest neighbors. (d) A random network of P atoms (intentionally connected), while M atoms are not shown for clarity.

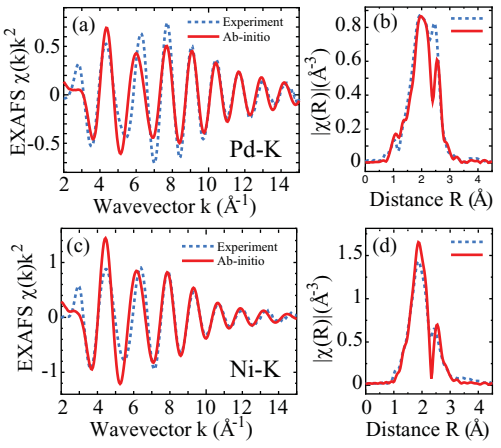

FIG. 2. (Color online) EXAFS spectra $k^2\chi(k)$ of $Pd_{40}Ni_{40}P_{20}$ BMG and the corresponding Fourier transforms at (a and b) Pd-K and (c and d) Ni-K edges obtained experimentally (broken lines) and from model calculations using the configuration of the simulated sample (full lines). The highest first peak in (b) represents Pd-P, while the second peak at ∼2.5 Å represents Pd-Pd(Ni) pairs. In (d), the highest first peak represents Ni-P, and the second peak at ∼2.5 Å represents Ni-Pd(Ni) pairs.

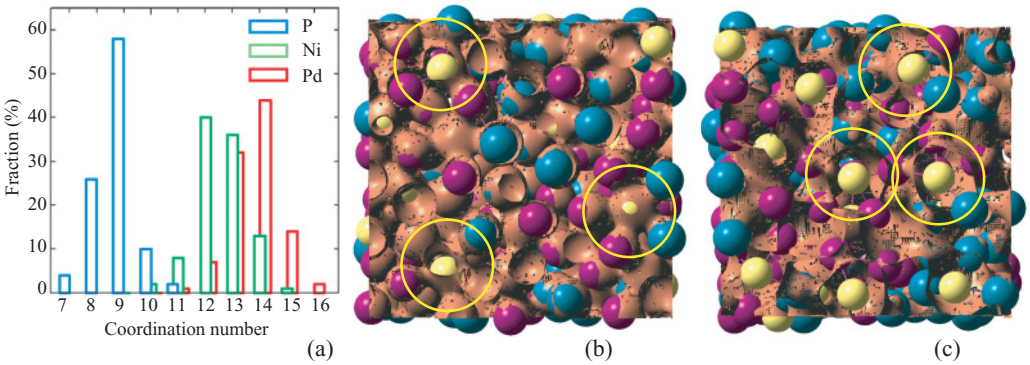

FIG. 3. (Color online) (a) Fractions of different nearest neighborhoods of Pd, Ni, and P atoms in the simulated $Pd_{40}Ni_{40}P_{20}$ BMG. (b) and (c) show the total charge density and the charge density in the energy range of the P-M bonding states, respectively. The latter shows charge accumulation between P and M atoms. Circles are drawn around some P atoms near the boundary of the simulation cell to show that the packing can be considered in terms of polyhedra around P atoms that are connected via M atoms. Pentagonal pyramid-type nearest-neighbor environment can be seen around the circled P atoms.

than the atomic fraction weighted sum of the cohesive energies, 3.97 eV/atom of the elemental solids of Pd, Ni, and P. Accordingly, the formation of Pd-Ni-P BMG is exothermic, and the heat of formation is calculated to be about 0.5 eV/atom. This is a large gain in energy, and it satisfies a criterion of BMG formation.[19]

In order to check if the simulated atomic structure of the Pd-Ni-P BMG could be considered as an ensemble of clusters, we studied the local neighborhoods of Pd, Ni, and P atoms. The distribution of the coordination values of Pd, Ni, and P atoms is shown in Fig. 3(a). For P, the coordination number lies in the range of 7 to 11, and the distribution peaks at 9 (capped tetragonal antiprism or tricapped prism type), while 8 (tetragonal antiprism or bicapped prism type) is the second best. Coordination 9 of P atoms with tricapped prism structure is well known in metal-rich phosphides,[20] and in the BMG phase, the prism structure is distorted, as shown in Fig. 4. For Ni atoms, the coordination ranges between 9 and 14, with the maximum number of Ni atoms having 12 coordination. Coordination 13 is also almost equally abundant, while for Pd, the largest atom in this BMG, the coordination ranges between 10 and 15, with the maximum number of Pd atoms having coordination 14, while 13 is less abundant. The increase in the number of nearest neighbors in going from P to Ni and then to Pd is expected due to the increase in the atomic size. A few representative nearest-neighbor environments with different numbers of Pd, Ni, and P atoms around Pd, Ni, and P sites are shown in Fig. 4, and the local environments for several P, Ni, and Pd atoms are given in Figs. A1–A3 in supplementary material.[21] In metallic systems, coordination 12 is often associated with icosahedral arrangement for close packing. However, our results show much disorder in the atomic arrangements around Ni and Pd atoms. In general, the distribution of the atoms around different Pd, Ni, and P atoms is not the closest packed due to covalent bonding between P and some M atoms. This is also seen from a large variation in the nearest-neighbor bond lengths, which are in the range of 2.28–3.00 Å and 2.12–2.80 Å, respectively, for Pd-P and Ni-P bonds. In the latter case, the distribution is strongly peaked at around 2.28 Å, and this is reflected in the form of a shoulder in $g(r)$ at small r in Fig. 1(b). Note that the first peak in the EXAFS spectrum at the Ni-K edge is narrower than the corresponding Pd-K edge peak. The nearest-neighbor Ni-Ni, Pd-Ni, and Pd-Pd bond lengths vary in the range of 2.36–2.98 Å, 2.49–3.10 Å, and 2.64–3.25 Å, respectively, and this is again in agreement with the EXAFS data. Our results show that *no two P atoms are nearest neighbors, and the distribution of nearest-neighbor P-P bonds has two peaks, one around 3.7 Å and the other around 4.5 Å*. Accordingly, the second major peak in $g(r)$ should have a significant contribution from such P-P pairs. In the case of $Ni_{80}P_{20}$ metallic glass, the atomic structure[12] also shows that P atoms are not nearest neighbors. Further, our calculations show that a large fraction of the 9-coordinated P atoms shows segregation of Ni atoms[21] (higher fraction of Ni than Pd atoms), while 8-coordinated P atoms have a maximum fraction characterized by an equal number of Ni and Pd atoms. On the other hand, 7-coordinated P atoms have segregation of Pd atoms. This behavior is understandable on the basis of the larger size of Pd atoms compared to Ni. Also, about 38 (50) Ni atoms in the sample have three (two) P atoms as nearest neighbors, while only 12 Pd atoms have 3 P as nearest neighbors.

In order to learn more about Ni-P and Pd-P bonding, we performed calculations on different-sized Ni clusters with a P atom at the center, as well as Pd clusters with a P atom at the center. It is found that the binding energy, defined as the difference in the energy of $P@X_n$ (X = Ni and Pd) cluster and the sum of the energies of P and n X free atoms, is much higher for $P@Ni_n$ clusters as compared to the values for $P@Pd_n$ clusters. Therefore, the P-Ni bond is energetically more favorable. This has been also confirmed from calculations on P-Ni and P-Pd dimers, which have binding energies of 3.326 eV and 2.560 eV, respectively. These results also support our finding of a higher number of P atoms around Ni and a larger number of Ni atoms around P atoms on the basis of favorable energy considerations. Furthermore, the P-M-P angles between the short P-M bonds lie in the

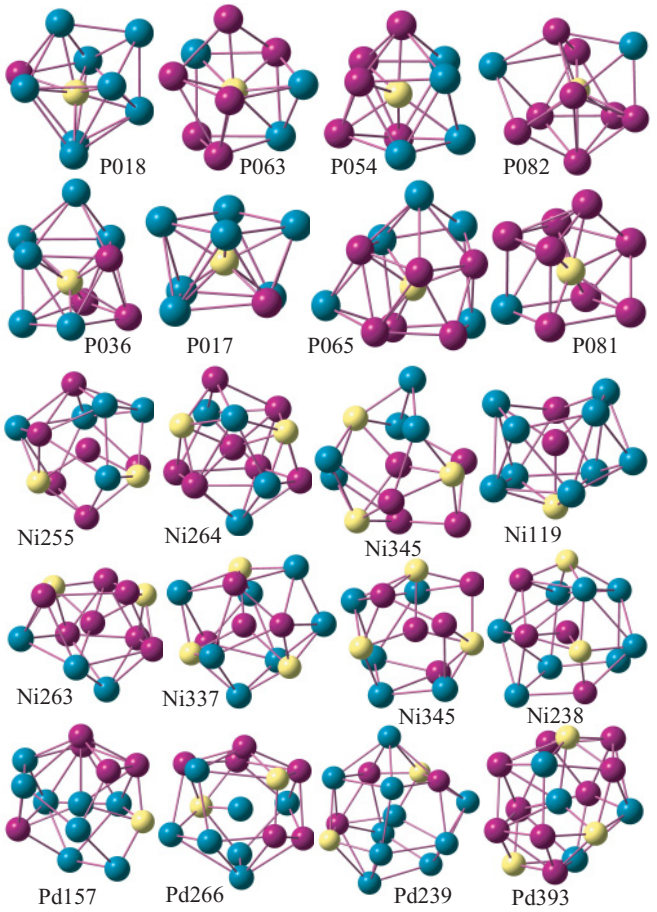

FIG. 4. (Color online) Atomic configurations of different nearest neighborhoods of P (yellow in color and light gray in print), Ni (violet in color and black in print), and Pd (dark blue in color and dark gray in print) atoms with high abundance in $Pd_{40}Ni_{40}P_{20}$ BMG sample. For P, 8- and 9-coordination polyhedra with tetragonal antiprism and capped tetragonal antiprism configuration can be seen, which can also be viewed as bicapped and tricapped prisms, respectively. The polyhedra around Ni and Pd atoms are more disordered. The notation Xlmn represents the number of neighbors of X atom with l P, *m* Ni, and *n* Pd atoms within a distance of 3.2 Å. Nanoscale clustering of like M atoms can be seen in many cases.

range of 103° to 130°, which can be understood in terms of *d-s* hybrids with angles of 116°34′, while some angles have the value of about 145°, which suggests involvement of *p* orbitals also. Such large angles are more frequently found around Pd atoms, and because of the wider extent of *5p* orbitals in Pd compared with *4p* orbitals in Ni, the formation of *d-s-p* hybrids is more likely around Pd atoms. The Ni-P-Ni, Ni-P-Pd, and Pd-P-Pd angles with short P-M bonds lie in the range of 106°–160°. Our results suggest that, in general, Pd-Ni-P BMG can be considered as an ensemble of polyhedral clusters centered on P atoms with neighboring polyhedra sharing M atoms. The short and strong P-M bonds form a random network [Fig. 1(c)], while the remaining Pd and Ni atoms act as metallic glue. The stronger interaction between P and some M atoms and its covalent character of bonding lead to less disorder around P atoms, while polyhedra around Pd and Ni atoms get more disordered to provide better bonding

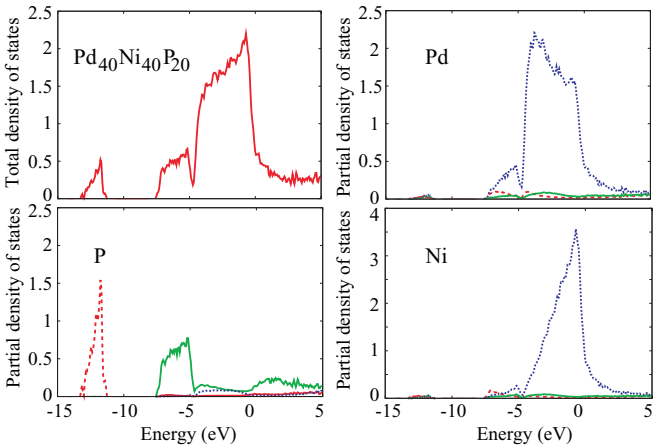

FIG. 5. (Color online) The total and the partial densities of states per atom for the simulated $Pd_{40}Ni_{40}P_{20}$ BMG. Zero of energy is the Fermi energy. Red (broken line), green (full line), and blue (dotted line) curves in the partial densities of states of P, Pd, and Ni show *s*, *p*, and *d* components, respectively. For Ni and Pd, the *s* and *p* components are very small. The partial densities of states for Pd, Ni, and P show states in the energy region of about −7.5 to about −5 eV, which are the bonding states with strong hybridization between the *p* orbitals of P and the *d* orbitals of Pd and Ni. One can also notice the *p* states of P above the Fermi energy and some contribution of *d* states of Pd and Ni in the same region, and these are the antibonding states.

of P atoms with those Ni or Pd atoms that have shorter P-M bonds.

B. Electronic structure

Figure 5 shows the total and the partial DOS of the $Pd_{40}Ni_{40}P_{20}$ BMG at 0 K. The states near the bottom of the *d* band arise mainly from the *p* orbitals of P and are the bonding states arising from the hybridization with Pd *4d* and Ni *3d* states. Similar results were obtained earlier using cluster calculations.[22] The Ni states lie closer to the E_F. The antibonding P-M (M = Pd and Ni) states lie just above the E_F, as it can be clearly seen from the partial DOS of P atoms. The strong contribution of Ni *3d* states just below the E_F agrees very well with the photoemission data[6] at 110 eV energy, in which the main emission arises from Ni atoms, and there is a peak just below E_F. Also, the photoemission at 50 eV energy has dominant emission from Pd atoms, and again our Pd partial DOS agrees very well with this experimental data. The overall total DOS obtained from our calculations also agrees very well with the experimental results, except for the relative heights of the peaks corresponding to Pd and Ni atoms, and this is due to the relative cross sections of Pd and Ni atoms at the photon energy used in the experiment.[6] The total DOS at E_F is much smaller as compared to that in bulk Pd and Ni, as also found in experiments, and it also satisfies a criterion for BMG formation.[7] The small number of *3d*-holes in Ni states could be filled if some of the Ni atoms in the metallic glue were replaced with Cu, which would make the DOS at E_F even lower and could enhance the stability of the BMG as observed.[23] Note that from our calculations on Cu-P and Ni-P

dimers, Ni has higher binding energy with P as compared to Cu. So, replacement of the Ni that binds with P very strongly is unlikely, while replacement of some Ni with Cu in the glue is also good, because it will enhance stability since the heat of formation of PdCu alloy is negative,[24] while PdNi has a tendency to phase separate, which we also find in our BMG atomic structure.

Further insight into the bonding behavior is obtained from the charge distribution shown in Fig. 3(b). In general, the bonding is metallic, but around P atoms, there is covalent bonding, as can be further seen in Fig. 3(c), in which the charge density isosurface has been shown by considering states in the energy range of −5.0 to −7.9 eV, where the P and M (Pd and Ni) bonding states lie. The charge density has high distribution in between a P atom and its surrounding polyhedron of Pd/Ni atoms. We have circled the atoms on the polyhedra around some P atoms, and one can see nearly touching circles. Accordingly, as discussed before, the BMG phase has P-centered polyhedra connected via a metallic glue of Pd and Ni atoms. Experimentally, the optimal fraction of P has been found[5] to be about 20%, and our results show that at this composition, all the P atoms are surrounded by metal atoms in the BMG phase. This could be a reason for the particular stability at this composition, but more calculations for different compositions of P would be helpful. The different sizes of Pd and Ni atoms and the different bonding with P, as well as the different bonding among Pd and Ni atoms, lead to inhomogeneities of Pd and Ni distribution at the nanoscale, as well as glass disorder. We also checked the difference in the charge density of the BMG sample and the sum of the charge densities of only Pd, only Ni, and only P atoms at the respective positions as in the BMG and found some charge transfer to P sites from the regions of Pd and Ni atoms.

IV. SUMMARY

In summary, the atomic structure of $Pd_{40}Ni_{40}P_{20}$ BMG has been simulated from *ab initio* calculations, and it agrees very well with the data obtained from EXAFS experiments. The calculated pair distribution function and the electronic structure are in excellent agreement with the available experimental results, suggesting that the obtained atomic structure of the Pd-Ni-P BMG is a good representation of the actual system. We find that the BMG can be considered to be formed of P-centered polyhedra that are interconnected, forming a random network of covalently bonded P-M-P bonds along with a metallic glue of remaining Pd and Ni atoms. No two P atoms are nearest neighbors, and this also sets an upper limit for the concentration of P atoms in an optimally bonded BMG of Pd-Ni-P that is about 20 at.%. The covalent bonding makes this glass not the closest packed, and the polyhedra around Pd and Ni atoms are quite disordered, with a tendency toward nanoscale clustering of like M atoms. We hope that the simulated structure will provide a basis to develop further understanding of the properties of this family of BMGs.

ACKNOWLEDGMENTS

V.K. gratefully acknowledges the hospitality at the International Frontier Center for Advanced Materials (IFCAM). We are thankful to the staff of the Center for Computational Materials Science for allowing the use of the Hitachi SR11000 super computer and their support. The EXAFS/XRD experiments are supported by the Japan Synchrotron Radiation Research Institute (JASRI)/SPring-8 under Proposals No. 2010A1029, No. 2010A1078, and No. 2010B1492.

*Corresponding author: kumar@vkf.in

[1] A. Inoue, K. Ohtera, K. Kita, and T. Masumoto, Jpn. J. Appl. Phys. **27**, L2248 (1988).

[2] H. W. Kui, A. L. Greer, and D. Turnbull, Appl. Phys. Lett. **45**, 615 (1984).

[3] A. Inoue, X. M. Wang, and W. Zhang, Rev. Adv. Mater. Sci. **18**, 1 (2008).

[4] Preliminary results were presented by V. Kumar, T. Fujita, M. W. Chen, A. Inoue, and Y. Kawazoe in APS March Meeting (2009), abstract X36.002.

[5] Y. He, R. B. Schwarz, and J. I. Archuleta, Appl. Phys. Lett. **69**, 1861 (1996).

[6] S. Hosokawa, N. Happo, H. Sato, M. Taniguchi, T. Ichitsubo, M. Sakurai, E. Matsubara, and N. Nishiyama, Mater. Trans. **46**, 2803 (2005).

[7] S. R. Nagel and J. Tauc, Phys. Rev. Lett. **35**, 380 (1975).

[8] S. O. Hruszkewycz, *The Effect of Fluctuation Microscopy Constraints on Reverse Monte Carlo Models of Metallic Glass Structure*, Ph.D. Dissertation (Johns Hopkins University, Baltimore, 2008); see [http://proquest.umi.com/pqdlink?did=1691646921&Fmt=7&clientId=85175&RQT=309&VName=PQD] (last accessed on 5 Oct' 2011).

[9] P. H. Gaskel, in *Glassy Metals II*, edited by H. Beck, H.-J. Guntherodt (Springer, Heidelberg, 1983), Chap. 1; A. S. Bakai, in *Glassy Metals III*, edited by H. Beck, H.-J. Guntherodt (Springer, Heidelberg, 1994), Chap. 6.

[10] D. B. Miracle, Nat. Mater. **3**, 697 (2004).

[11] T. Fujita, K. Konno, W. Zhang, V. Kumar, M. Matsuura, A. Inoue, T. Sakurai, and M. W. Chen, Phys. Rev. Lett. **103**, 075502 (2009).

[12] H. W. Sheng, W. K. Luo, F. M. Alamgir, J. M. Bai, and E. Ma, Nature **439**, 419 (2006).

[13] E. A. Stern, M. Newville, B. Ravel, Y. Yacoby, and D. Haskel, Physica B **208–209**, 117 (1995).

[14] G. Kresse and D. Joubert, Phys. Rev. B **59**, 1758 (1999).

[15] P. E. Blöchl, Phys. Rev. B **50**, 17953 (1994).

[16] J. P. Perdew, in *Electronic Structure of Solids* '91, edited by P. Ziesche and H. Eschrig (Akademie, Berlin, 1991).

[17] O. Haruyama, Intermetallics **15**, 659 (2007).

[18] A. L. Ankudinov, B. Ravel, J. J. Rehr, and S. D. Conradson, Phys. Rev. B **58**, 7565 (1998).

[19] A. Inoue, Acta Mater. **48**, 279 (2000); A. Takeuchi and A. Inoue, Mater. Trans. JIM **46**, 2817 (2005).

[20] R. Pöttgen, W. Hönle, and H. G. von Schnering, *Phosphides; Solid-State Chemistry, Encyclopedia of Inorganic Chemistry* (Wiley, Weinheim, 2006).

[21] See Supplemental Material at http://link.aps.org/supplemental/10.1103/PhysRevB.84.134204 for the local environments of several P, Ni, and Pd atoms that are given in Figs. A1–A3.

[22] T. Takeuchi, D. Fukamaki, H. Miyazaki, K. Soda, M. Hasegawa, H. Sato, U. Mizutani, T. Ito, and S. Kimura, Mater. Trans. JIM **48**, 1292 (2007).

[23] N. Nishiyama, and A. Inoue, Mater. Trans. JIM **37**, 1531 (1996); Appl. Phys. Lett. **80**, 568 (2002).

[24] F. R. de Boer, R. Boom, W. C. M. Mattens, A. R. Miedema, and A. K. Niessen, *Cohesion in Metals: Transition Metal Alloys* (Elsevier Science Publisher B. V., Amsterdam, 1988).